Accepted Manuscript

Methods of fabricating Cu-Al-Ni shape memory alloys

Ashish Agrawal, Ravindra Kumar Dube

Please cite this article as: A. Agrawal, R.K. Dube, Methods of fabricating Cu-Al-Ni shape memory alloys, *Journal of Alloys and Compounds* (2018), doi: 10.1016/j.jallcom.2018.03.390.

Methods of fabricating Cu-Al-Ni shape memory alloys

Abstract

Recently Cu-Al-Ni shape memory alloys have gained special attention due to their high temperature applications. This article attempts to formulate the various processing routes for processing of Cu-Al-Ni shape memory alloys such as casting route, powder metallurgy route, rapid solidification and spray forming process. The pros and cons of various processes are provided in detail. The additive manufacturing, which is an emerging process is discussed which could be a promising technique of preparing Cu-Al-Ni shape memory alloys. Further recommendations are provided in terms of producing fine-grained near net shaped shape memory alloys for high temperature applications.

Keywords: Cu-Al-Ni shape memory alloys; casting route; powder metallurgy; rapid solidification; spray deposition, selective laser melting.

Introduction

Shape memory alloys (SMAs) are an exquisite class of active materials with an ability to regain its original shape at high temperatures. There is a wide range of alloys which exhibit the shape memory effect, but only those alloys are commercially attractive which show a substantial amount of strain recovery and generate significant force due to shape change. Among the Cu-based shape memory alloys, Cu-Al-Ni alloys have a higher thermal stability than Cu-Zn-Al alloys [1, 2]. Therefore, Cu-Al-Ni alloys are being developed for high temperature applications due to their potential to be used as sensors and actuators at temperatures around 200 ⁰C. On the other hand, Cu-Zn-Al alloys have maximum working temperatures of 120 ℃, but they sh ow better ductility as compared to Cu-Al-Ni alloys for low temperature applications [2].

Shape Memory Effect (SME) is shown by alloys exhibiting crystallographically reversible thermo-elastic martensitic transformation. At a higher temperature, the same alloys have another unique property called as super-elasticity [3]. Superelasticity is caused

due to large non-linear recoverable strain (up to 18%) upon loading and unloading, in which a specimen once deformed by application of force regain its original shape automatically without any application of heat [1]. The Ni-Ti, ferrous alloys and Cu-based alloys are considered as practical materials for applications among many shape memory alloys. Ni-Ti alloys, an equi-atomic compound of Ni and Ti, are the most widely used shape memory alloys. They show excellent shape memory strain up to 8 % and are thermally stable. However, the reactivity of Ti limits their processing in air and hence all melting operations are to be carried out in vacuum. In recent decades, Cu-based shape memory alloys have emerged as a potential material for variety of applications, such as high damping material, sensors and actuators. Cu-Al-Ni shape memory alloys have gained special attention due to their high thermal stability among the other Cu-based shape memory alloys. The presence of SME, thermo-elastic martensitic transformation and crystallography in the Cu-Al-Ni alloy was confirmed by Otsuka [4-6]. Some ferrous alloys also exhibit SME under certain conditions [7]. Fe-Mn-Si alloys are the most important iron-based shape memory alloy. However, they can recover shape memory strain less than 4 %.

Types of shape memory effects

An alloy is said to exhibit one-way SME when it is deformed at a temperature below the critical temperature, and recovers its original shape on heating above the critical temperature. When the alloy cools down, it retains the original un-deformed shape and must be further deformed to obtain the SME. Figure 1 shows the schematic process of testing the shape memory effect on a specimen. The one-way SME is shown by the alloy can thus remember its original un-deformed shape but should be assisted mechanically every time to demonstrate the SME [8].

An alloy is said to exhibit the two-way SME, when it remembers two different shapes: one at a low temperature and the other at the high temperature. A material that shows a shape memory effect both during heating and cooling is called two-way shape memory alloy. This effect can also be obtained without the application of an external force which is known as intrinsic two-way effect. SMAs also exhibit super elasticity in which a small amount of force induces deformation, but when the force is removed, the material

automatically recovers its original shape, without heating. One of the few applications is in indestructible spectacle frames which can be bent and twisted and recover their original shape after the removal of the deforming force [8].

Crystal structures of austenite and martensite phase

Cu-based shape memory alloys have superlattice structures. The parent phase has superlattices associated with the body-centered cubic structure (B.C.C.) and these are classified as β-phase alloys. [9] The parent austenitic phase (β) is divided into two types according to the superlattice or composition ratio. The parent phase denoted by β_2-phase, exists as B_2 type in Ni-Ti alloys and has elemental composition in the ratio about 50:50. The parent phase denoted by β_1-phase, exists as DO_3 type in Cu-based SMAs and has about elemental composition in the ratio about 75:25.

The martensitic phases of the β-phase alloys also have superlattice structure like the parent austenitic phase. During martensitic transformation, the parent phase undergoes deformation by shearing, and the resulting structure can be obtained by stacking of the 6 atomic planes (A, B, C, A', B', C') which are shown in figure 2. Thus, depending upon the stacking of these planes, different types of martensitic structures are obtained. The B_2 type parent phase transforms to 2H, 3R and 9R martensites, while the DO3 type parent phase transforms to 2H, 6R and 18R martensites on quenching [9].

The different stacking of the six planes result in the formation of various martensitic structures such as 2H, 3R, 6R, 9R and 18R. Figure 3 shows the periodic stacking of the planes, which show a twinned structure, which is necessary for the realization of shape memory effect. Depending upon the stacking of the planes, these are termed as 2H, 3R, 6R, 9R and 18R.

Martensitic transformation

The Martensitic transformation (MT) is not a new phenomenon, but was first observed a few decades back, to describe the hard-micro-constituent formed when steels are heat treated at a high temperature followed by quenching [10]. Martensite was originally used in 1895, after the German Scientist Adolf Martens, to describe the hard and brittle phase

thus formed [11]. Usually the parent or austenitic phase is cubic and the product or martensitic phase has a lower symmetry. However, the MT in most iron and steels are not crystallographically thermo-elastic, hence does not exhibit the SME. The SME and SE in SMA are realized due to the crystallographically reversible MT. The SMAs have a characteristic feature of strain-induced MT which is capable of temperature reversion. MT is accompanied by a shape change in addition to the volume change common to most phase transformation in metals and alloys [12]. MT are characterized as a diffusionless solid-state phase transformation, in which atoms move in a coordinated manner, often by a shear-like mechanism, when temperature is lowered below a certain critical temperature. The phase change involves a definite orientation relationship because atoms move co-operatively. Moreover, the product phase bears a well-defined crystallographic relationship with the parent phase. They are sometimes also referred to as shear or displacive transformation or military transformation. Though the relative displacement of atoms is small, a macroscopic shape change appears associated with MT to accommodate the shear. These small coordinated movements of atoms result in the formation of a new twinned martensite structure [10]. A special feature of MT is that each colony of martensite laths/plates consists of a stack, called the correspondence variants of the martensite, as they have the same structure, but their orientations are different.

Mechanism of shape memory effect

The SME is a phenomenon in which a specimen, deformed below M_f or between M_f and A_s temperature, regains its original shape by reverse transformation on heating above A_f temperature. Figure 4 shows the shape memory effect at an atomic level. Otsuka demonstrated the origin of shape memory effect in Cu-14.2Al-4.3Ni alloy [4-6]. According to which, the deformation mode in the martensitic state is twinning rather than slip. The plastic deformation is effected by the growth of twins that are favorably oriented and by the destruction of twins that are unfavorably oriented. A reverse transformation occurs, when a specimen earlier deformed below A_s temperature, is subsequently heated above A_f temperature. During the reverse transformation, all the twins are annihilated, whether they are formed by transformation or by application of

external stresses. In order to keep the habit plane between matrix and martensite to be invariant, twins are created when the habit plane move towards the matrix upon MT and when the habit plane move towards the martensite upon reverse transformation twins are annihilated.

Transformation hysteresis

Figure 5 shows a typical heating and cooling curves of a shape memory alloy. The heating and cooling curves do not overlap and the alloy is said to exhibit hysteresis. M_s and M_f are the martensite start and finish temperatures respectively, and A_s and A_f are the austenite start and finish temperatures respectively. When a SMA is deformed below M_f and subsequently heated above A_f, the original shape is regained. On cooling, the parent austenite phase transforms to martensite phase, which can be deformed to show shape memory effect. The hysteresis width T, represents the frictional resistance of the alloy to convert from martensitic phase to austenitic phase. The hysteresis width of the SMAs varies with alloy composition and is typically varies in the range of 10-50 ˚C [13].

Requirements for exhibiting shape memory effect

It can be deduced from the above discussion that following characteristics are necessary in an alloy for the realization of shape memory effect: -

1. The parent austenitic phase must have an ordered structure, i.e. DO3, B2 type, which exhibit crystallographically reversible transformation from product phase back to parent phase. An ordered structure means that there is an appreciable amount of resistance to dislocation motion to avoid irreversible deformation. Dislocations in the austenitic phase provides site for heterogeneous nucleation.
2. The austenite to martensite phase change must be accompanied by a small volume change.
3. The martensite should self-accommodate the strain with the help of twinning. An ordered structure is favorable for avoiding slip, because they usually have a higher critical stress for slip than that for a disordered structure.

Applications of shape memory materials

Shape memory materials are gaining attraction for potential applications because of their reliability and multi-functionality. They have attracted great deal of interest in wide variety of applications such as aerospace applications, medical applications, automobile applications, civil engineering applications, a few of them have been mentioned below:

1. Shape memory alloys are used as pipe and tube couplings as aircraft hydraulic couplings. It came to practical applications for the first time on an Agrumman F-14 fighter plane. The couplings are made at cryogenic temperatures in the martensitic state. On heating the joint, the alloy regains its original shape, but is constrained by the pipe. The stress developed causes a strong joint in the coupling (Figure 6 (a)) [13].

2. Shape memory alloys can be used in fire sprinkler system and fire safety valve, which gets activated by shape change caused by heating on fire. They can be used as electric circuit breaker (Figure 6 (b)) [14].

3. Shape memory alloys are used as sensors and thermal or electrical actuators impact absorption in automobiles (Figure 6 [c]) [14].

4. Shape memory alloys are used for medical applications such as Simon filters in cleaning the arteries of heart and spacers in connecting the knee joint (Figure 6 [d] & 6 [f]) [4].

5. Shape memory alloys are also used as fastener rings. They can also be used as pseudo-elastic eye glass frame (Figure 6 [e]) [14].

6. Shape memory alloys can also be used in the robotic applications such as connectors in robotic arms (Figure 6 [g]) [15].

Phase diagram of Cu-Al-Ni system

Figure 7 shows phase diagram of the Cu-Al-Ni ternary alloy system at 3 wt % Ni [1, 16]. For the alloy to exhibit shape memory effect, the Al content should be such that the material exists as single β-phase at high temperatures. The Cu-Al-Ni alloys can only be hot worked in the β-phase region. Usually the practical transformation temperature in

Cu-Al-Ni alloys is achieved when the Al content lies in the eutectoid or hyper-eutectoid regions [2].

The β-phase in the binary Cu-Al alloy system undergoes a eutectoid transformation at 565 °C into α-phase (F.C.C.) and the brittle γ_2-phase (Cu_9Al_4 cubic phase). The presence of ternary element Ni retards the eutectoid transformation into α and γ2. Ni also shifts the Cu-Al eutectoid to higher Al content. Since the alloys become brittle with increasing Ni content, the content of Ni should be kept around 4 wt %. When the Cu-Al-Ni alloys are quenched from the β-phase, it transforms into β', β' + γ' or γ' martensites depending upon the Al content. The β' martensites are formed at lower Al content, while higher Al content results in the formation of γ' martensites. Excellent shape memory effects are observed in alloys with Al content close to 14 wt. %, for which the M_s temperature lies in the room temperature range [14].

The present review covers the preparation of Cu-Al-Ni shape memory alloys developed for making metal strips by various routes.

Processing routes of Cu-Al-Ni SMA

In recent decades, Cu-based SMAs have emerged as a potential material for variety of applications, such as high damping material, sensors and actuators. Cu-Al-Ni SMAs have gained special attention due to their higher thermal stability in relation to other Cu-based SMAs. However, the large grain size, large orientation dependence of the transformation strain, large elastic anisotropy and grain boundary segregation, deteriorates the mechanical properties in polycrystalline Cu-Al-Ni alloys which make them susceptible to intergranular fracture. This renders them unsuitable for widespread practical applications.

1. **Casting Route**

Manufacturing method involving casting is one of the most common methods for preparing SMAs. In conventional casting route, Cu-Al-Ni SMAs are prepared as described below. High purity Cu, Al and Ni are melted in an induction furnace under an inert atmosphere and cast into ingots in a mould. The Cu-Al-Ni alloy are then

homogenized and mechanically worked (such as hot-rolled) to produce plates or stripes. Several efforts are made in developing fine grained Cu-Al-Ni alloys with improved ductility and superior mechanical properties. However, the conventional casting route for preparing Cu-Al-Ni SMA produces coarse grain structure. As a result, the Cu-Al-Ni SMAs produced by casting route are brittle, and are susceptible to intergranular cracking, leading to their limited potential applications. The conventional casting method for preparing Cu-Al-Ni shape memory alloy suffers from a disadvantage that it produces coarse grain structure of the order of 1 millimeter. Therefore, the brittleness is a severe problem in cast Cu-Al-Ni alloys due to large grain size combined with large elastic anisotropy.

1.1 Conventional casting route without quaternary addition

Leu et al [17] has prepared Cu-13.8Al- 3.8Ni (wt %) alloy by casting route involving induction furnace melting under argon atmosphere. The cast alloys were hot-rolled to produce plates of 1.2 mm thickness. The rolled specimens after solution treatment at 1123K for 10 min and water quenching exhibited a grain size of about 460 µm as shown in figure 7. The fracture strain and fracture strength of the Cu-Al-Ni alloy were reported to be 0.8% and 260 MPa respectively. Figure 8 shows a typical SEM microstructures of the Cu-13.8Al-3.8Ni (wt %) and Cu-13.8Al-4Ni-0.2Cr (wt %) obtained after solution treatment at 850 °C followed by water quenching. Roh et at [18] prepared Cu-13.4Al-3.8Ni (wt %) in an induction furnace. The cast alloy was hot rolled in stages to achieve a final thickness of 2 mm. The rolled Cu-Al-Ni alloy homogenized at 1123K exhibited a grain size of the order of 2300 µm and possess weak mechanical properties. Miyazaki et al [9] prepared Cu-14Al-4Ni alloy by melting Cu, Al, Ni in an induction furnace under an argon atmosphere and casting into mould. The cast alloy was subsequently annealed at 1273K for 1 hr and quenched into water of different temperatures. It is reported that the samples quenched in boiling water showed highest fracture stress of 240 MPa. Though the fracture stress has improved with the increase in the temperature of the quenching media, however the desired level of grain size could not be attainable which resulted in a fracture strain of 1% in all the cases. Duerig et al [19] has prepared Cu-14.2Al-3.2Ni alloy by casting route. The alloy exhibited a grain size of the order of

1500 μm and showed a fracture stress of 440 MPa coupled with a weak fracture strain of 0.6%. Sure and Brown et al [20] has prepared the Cu-14.2Al-3.2Ni alloy in high frequency induction furnace under an argon atmosphere. The alloys were preheated at a temperature of 1123K and subsequently hot-rolled to strip of 1 mm thickness. The reported grain size of the hot-rolled and recrystallized alloy at 1123 K shows large variation of grain size, even as large as 750 μm is reported that exhibit a weak fracture stress of 150 MPa and a fracture strain of 2%. Sure and Brown et al. [20] has reported that when β-phase Cu-Al-Ni SMA are cold worked by 10% and then heated at 1073 K, recrystallization and grain growth takes place even in the case of Cu-Al-Ni-Ti SMA. Further by reducing the annealing temperature to 1023 K, the cold-rolling process; instead of retarding the grain growth, leads to cracking of samples due to the continuous precipitation of second phase particles at the grain boundaries. Therefore, it is suggested to immediately quench the Cu-Al-Ni SMA after the final rolling pass is over to retain the high temperature deformation structure which would reduce the effect of recrystallization.

It is envisaged that when the liquid Cu-Al-Ni alloy solidifies at a slow cooling rate, the resulting bigger grain size are resulted, In order to control the grain size during casting process faster cooling rate may result is complete martensitic transformation. Oishi and Brown [21] et al. has reported the preparation of Cu-Al-Ni SMA by melting the pure Cu, Al and Ni in induction furnace. The alloy is chill cast in copper mould and subsequently hot rolled at 850 ˚C to produce a strip of 0.762 mm thickness. The grain size of the finished strip was reported to ~ 200 μm. The strain of 5.6% and 2.6% were observed in single crystals and polycrystalline specimens simultaneously. Mukunthan and Brown [22] have reported the preparation of Cu-Al-Ni in induction furnace which is subsequently cast and homogenized for 24 hours at 900 ˚C. This is subsequently hot rolled at 800 ˚C to a thickness of 4.3 mm which exhibited a grain size of 250 μm and a fracture stress of 650 MPa coupled with a fracture strain of 5%. Gama [23], has attempted to study the effect of Thermo-Mechanical Treatment on Mechanical Properties & Microstructure for (Cu-Al-Ni) Shape Memory Alloy. Abbas et al [24] has recently reported the melting of pure Cu, Al, and Ni in vacuum induction furnace in an inert argon atmosphere to produce a cast Cu-Al-Ni alloy. The alloy was subsequently

homogenized at 900 °C for 30 min and quenched in ice brine solution. Further the effect of thermo-mechanical treatment on the microstructure and mechanical properties of Cu-Al-Ni SMA alloy was studied in varying temperature. It was found that the shape memory effect was improved with increasing the temperature at which thermo-mechanical treatment was carried out.

1.2 Conventional casting route with quaternary addition

In Cu-Al-Ni ternary alloy, a prolonged solution treatment leads to dissolution of the second phase γ_2 precipitates and thus during the grain growth stage the second phase precipitates loses its effect of hindering the grain growth rate. This subsequently leads to the formation of a single β-phase microstructure that progressively results in increasing the grain growth. The grain size in Cu-Al-Ni alloys can be controlled by addition of quaternary elements that form precipitates rich in quaternary element that retards the grain growth. The presence of second phase precipitate in the matrix phase hinders the grain growth because of the grain boundary pinning effect caused due to the interaction of the grain boundary with the particle and therefore has pronounced effect in reducing the grain size. Casting using addition of quaternary element such as Cr, Ti, Cr, Zr, V or B has shown a significant improvement in the mechanical properties of the Cu-Al-Ni alloy [25]. Roh et al [18] has reported the effect of microalloying addition that resulted in improving the mechanical properties in the Cu-Al-Ni SMA. The fracture strength of Cu-Al-Ni alloy was increased from 380 MPa to 903 MPa and fracture strain was increased from 4% to 8.6% by addition of Ti and Zr as quaternary element in the base Cu-Al-Ni SMA. The increase in the strength is attributed to the refinement of grain size from 2300 μm to 290 μm and the presence of precipitates within the grains in the SMA. Lee and Wayman et al [25] has reported that the addition of quaternary element changes the mode of fracture from intergranular to transgranular.

However, compositional control during casting and limitations to achieve the desired level of grain size restricted further development of the alloy. Attempts are made to refine the grain size of alloy, the cast Cu-Al-Ni alloy ingot was re-melted with addition of 0.2 wt. % Cr. The fracture strain and fracture strength of the Cu-Al-Ni-Cr alloys were improved to 3.8% and 666 MPa respectively, but the grain size remained 460 μm.

Therefore, limitations to achieve the desired level of grain size and compositional control restricted further development of the alloy [25, 26, 27, 28].

2. Powder Metallurgy Route

Powder metallurgy route has emerged as an important alternative to the conventional "continuous slab casting – rolling" route for preparing metal strips. The starting material for powder metallurgy routes is metal or alloy powder. The various variants of powder metallurgy route for making metal strips have been discussed in detail by Dube [29]. It is well established that such routes have potential to reduce the energy requirements and capital equipment costs. However, their commercial application has been hindered, primarily due to the higher cost of starting metal powders. The powder metallurgy route provides better compositional control during processing and, fine grained material as compared to the conventionally casting produced counterparts. During the last few years, attempts have been made to develop Cu-Al-Ni alloys by powder metallurgy route starting from elemental powders or pre-alloyed powder. Particularly, mechanical alloying has emerged as a promising method to produce a variety of nanocrystalline and ultra-fine-grained powders. The consolidated Cu-Al-Ni preforms are densified by sintering, hot isostatic pressing, hot pressing, mechanical working or a combination of these processes. The flowchart of the unit-steps involved in the formation of alloy strip are shown in figures 10 and 11.

2.1 Mechanical alloying followed by sintering process

Tang et al. [30] prepared Cu-14Al-4Ni (wt %) alloys by mechanical alloying, followed by compaction and sintering. The elemental powders were mechanically alloyed for 40 hours in argon atmosphere using planetary ball to powder ratio of 5:1. The mechanically alloyed powders were pressed at 900 MPa into a disc shape preform. The preforms were subsequently sintered at 950 °C for 20 hours in an argon atmosphere. The sintered specimens were then solution treated at 900 °C and water quenched at room temperature. Further, the study on the effect of mechanical alloying on microstructure and properties of Cu-Al-Ni shape memory alloy is carried out. The shape memory properties of the final alloy showed poor properties with 68 % shape recovery for the

first thermo-mechanical cycle and 30 % shape recovery for the second thermo-mechanical cycle. Moreover, the shape memory properties were evaluated at a pre-strain of 1 %. Such a low value of strain recovery was due to the internal cracks and residual porosity in the final alloy. Furthermore, the processing route is commercially unattractive due to the poor shape memory properties, and milling time in inert gas atmosphere for a longer period. Therefore, it is believed that only sintering cannot produce the high-density material. So, the mechanically alloyed powders were consolidated using other processing methods to improve the shape memory properties.

2.2 Mechanical alloying followed by hot pressing and extrusion process

It is envisaged that mechanical alloying followed by hot pressing could eliminate the porosity and produce the near net shape product. This process consists of mechanical alloying of the elemental powders followed by vacuum hot pressing and hot extrusion. In the mechanical alloying process, a high energy planetary ball mill is used in an inert atmosphere. This is followed by either vacuum hot pressing or hot isostatic pressing and hot extrusion. Rodriguez et al. [31] prepared Cu-14.2Al-4.2Ni wt. % alloy strips staring from pre-alloyed powders, followed by hot isostatic pressing and hot rolling. The pre-alloyed powders were hot isostatic pressed at 850 °C at 140 MPa compaction pressure. The consolidated preforms were subsequently hot rolled. The final strips were annealed at 900 °C for 30 minutes and ice quenched. The final strips were reported to show improved ductility due to formation of sub-grain structure on hot rolling. The shape memory recovery obtained from this alloy was 100% for about 100 cycles which showed a significant improvement compared to sintering of the pre-alloyed powders. However, the authors have not reported the details of hot rolling conditions. Moreover, the gas atomization and hot isostatic pressing makes the process expensive and commercially unattractive. The shape memory recovery obtained from this alloy was 100% for about 100 cycles which showed a significant improvement compared to sintering of the pre-alloyed powders. Xiao et al [32] have also shown that the hot pressing and extrusion process produces a chemical homogeneous material with near full density.

2.3 Mechanical alloying of pre-alloyed powders followed by hot isostatic pressing

This process consists of melting of the pure Cu, Al and Ni powders in the induction melting furnace followed by the gas atomization. This atomized powder is mechanically alloyed in a ball mill. This mechanically alloyed powder is then subjected to hot isostatic pressing to obtain the final alloy. A. Ibarra et al. [33] have confirmed that mechanical alloying before the hot isostatic pressing compaction is very beneficial for obtaining the final alloy with the desired martensitic transformation temperatures, as well as hysteresis and transformation width compared to the directly hot isostatic pressed pre-alloyed powder. In this process, the powders in the required composition are first gas atomized then compacted by hot isostatic pressing and then finally hot rolled. Hot rolling breaks up the oxide layer present on the powders and form a better metal to metal contact. Hot rolling also produces a sub grain structure. The presence of the sub grains allows the distribution of the stress at the grain boundaries. Sub-boundaries are composed of the arrangement of the super dislocations and can absorb moving dislocation when stressed. Thus, there is an increased amount of the plastic deformation before the fracture occurs, improving the shape memory properties of the alloy.

However, it is interesting to note that the vacuum hot pressed compacts were encapsulated in copper before hot extrusion and such an encapsulation makes the consolidation process complex. Mechanical alloying suffers from the disadvantage of high milling time and the requirement of inert atmosphere during milling. The powder metallurgy route can become economically more attractive if the route is based on mechanically mixed elemental powders of Cu, Al and Ni. Although the Cu-Al-Ni alloys have not been processed from the elemental powders but Dericioglu et al. [34] have attempted to process a Cu-Zn-Al alloy using the elemental powders.

2.4 Mechanical alloying of elemental and pre-alloyed powders followed by sintering and hot rolling

The powder metallurgy route employs mechanical alloying of elemental powders in ball mill in an inert gas atmosphere to produce Cu-Al-Ni alloy powder. The morphology and structural evolution of the Cu-Al-Ni elemental powders are studied in detail by Vajpai et al [35] at various stages of milling. Although the mechanical alloying could result in

better chemical homogeneity, but the prolonged milling time of 40h to 200 h makes the process inefficient. The powder metallurgy route could become viable if the mechanical alloying step is replaced by a more practical approach of mechanically mixing the elemental powder and eliminating the high milling time consumed in mechanical alloying. Sharma [36-37] et al has reported the preparation of Cu-Al-Ni SMA strips by hot rolling of sintered powder preforms from mechanical mixing of elemental Cu, Al, Ni powders in the ratio 82:14:4 (wt.%). The premixed Cu-Al-Ni alloy powders is subsequently cold compacted, followed by sintering at 873 K and hot rolling by reheating the sintered preforms at 1273 K. The hot rolled Cu-Al-Ni strips are homogenized at 1173 K for 4 hours and water quenched at room temperature which exhibited fracture strength of 476 MPa and a fracture strain of 5%. Also, the hot rolled strip is reported to show 100% shape recovery after 10 thermo-mechanical cycle. In this study the starting material Al used is air-atomized, and therefore it is believed that the presence of Al_2O_3 particles in the grain boundary might have restricted the full densification of the Cu-Al-Ni strip and has therefore lead to the poor mechanical properties.

To improve the Cu-Al-Ni SMA strips with improved mechanical property, further Vajpai [38] et al has attempted for the preparation of Cu-Al-Ni SMA strips by hot densification rolling of sintered powder using argon atomized pre-alloyed Cu-Al-Ni powder and using water atomized per-alloyed as starting material. The final hot rolled and homogenized Cu-Al-Ni strip exhibited an average grain size of 27 µm with improved fracture stress of 626 MPa coupled with a strain of 13.5%.

3. Rapid solidification processing

Rapid solidification method produces nearly net shaped material in the form of thin ribbons compared to casting which requires further machining to form the final alloy. Figure 9 depicts the experimental set-up of a free jet melt spinner and microstructure obtained in the rapidly solidified Cu-Al-Ni alloy [16]. Rapid solidification processing offers a convenient and economical production technology combined with the possibility of improving the mechanical properties of Cu-Al-Ni SMA through grain refinement. Rapid solidification processing has the advantage of producing thin ribbons directly from

the molten metal which does not require further thermo-mechanical treatment as required in conventional casting route. Moreover, the alloy produced exhibits homogenous microstructure due to the rapid cooling rate obtained during rapid solidification compared to conventional casting method. Several attempts were made in developing Cu-Al-Ni SMA by rapid solidification processing. Rapid solidification processes, such as melt spinning and twin roll casting, has potential to produce Cu-Al-Ni thin ribbons of about 80 µm thickness directly from the molten metal in a single step. Morawiec [39] produced 5 to 10 mm wide and 30 to 80 µm thick Cu-Al-Ni ribbons using melt spinning process. The alloys were melted in an induction-vacuum furnace. The alloys were subsequently melt-spun under an argon atmosphere with ejection pressure of 0.02 MPa onto a rotating copper wheel of 400 mm diameter. The wheel speeds used were in the range of 8 to 32 m/s. Morawiec [39] studied the changes in microstructure and mechanical properties of Cu-Al-Ni alloy ribbons with the change in wheel speed. The microstructure of the ribbons changes from fully martensitic through a mixture of 18 R + β_1 to the pure β_1 with the increase in the wheel speed with the simultaneous refinement in grain size. The ribbons produced with a wheel speed of 20 m/s exhibit good mechanical properties, high shape recovery under 40 MPa load and better resistance to thermal degradation. However, the relevant microstructures were not shown anywhere.

Goryczka [40] obtained Cu-Al-Ni alloy ribbons by melt spinning process. The bulk material was melted in an induction-vacuum furnace. The ribbons were manufactured using melt spinning process under argon atmosphere with ejection pressure of 0.02 MPa and wheel velocity of 19 m/s. The ribbons exhibited two-way SME. The degradation of the SME between first and third cycle was measured by the difference in % elongation, which was reported as < 0.1%. A maximum of 4.4% elongation has been reported after third cycle. Annealing at 900˚C for 20 min further increased the shape recovery with the increase in elongation. However, a significant degradation in SME was observed simultaneously. Lojen [16] melt-spun Cu-Al-Ni ribbons containing 13, 14 and 15 wt. % Al in a free jet melt spinner under a protective argon atmosphere. The grain size of the obtained ribbons was in between 20-50 µm. The ribbons were annealed at 800-850 ˚C for 90 s and subsequently water quenched. The water

quenched ribbons showed martensite structure with improved ductility on addition of boron to the master alloy. Malarria [41] produced thin ribbons and strips of Cu-13Al-5-6Ni-1Ti alloy using two different rapid solidification processes: [a] Melt Spinning (MS) and [b] Twin-Roll Casting (TWC). The alloy was melted in a quartz crucible under helium atmosphere in a high frequency furnace. The molten alloy was ejected with an argon pressure of 250 millibar, onto a rotating MS copper wheel of 400 mm diameter rotating at 19 m/s or between the two wheels rotating in opposite directions in TWC. The products obtained were ribbons and stripes, respectively from MS and TWC processes. Subsequently annealing was done at 700° C for 40 min for ribbons and for 1 h for tapes, followed by water quenching in room temperature for both cases. An average grain size of <2 μm was observed in as-cast ribbons and remained nearly same even after heat treatment. The maximum recoverable strains of 1.8% for ribbons and 1.4 to 1.8% for strips were reported in cyclic test under 90 MPa. It is reported that the strips obtained by TRC exhibited a higher tensile strength than ribbons however; the relevant details were not reported. The microstructure contained 18R structure in strips and 18R & 2H structures in ribbons as confirmed by TEM study.

Sobrero [42] obtained 12 mm wide and a 400 μm thick Cu–13Al–5Ni–1Ti (wt. %) strips by twin roll casting. The molten alloy superheated to 1250 °C was ejected at a pressure of 250 millibar from a quartz nozzle between two opposite rotating rollers with 400 μm diameter and a 10-mm thick copper rim under helium atmosphere. The prepared strips were homogenized by annealing at 900 °C for 60 minutes followed by ice water quenching. This treatment changed the secondary phase precipitate size and size distribution, and increased the shape recovery to values of 3.6 %. **Figure 2.11:** (a) Experimental set-up of a free jet melt spinner and (b) Microstructure obtained in the rapidly solidified Cu-Al-Ni alloy [16]. The rapid solidification processing suffers from disadvantage that it introduces internal stresses in the material which can impede the growth of the martensitic plates. This effect deteriorates the shape memory properties. The precipitation of intermetallic phases also occurs during rapid solidification processing. Therefore, there are microstructural variations present in the rapidly solidified alloy which in turn will increase the hysteresis loop of the alloy. However, with proper annealing time and temperature some alloys have shown about 3.6 % shape

recovery. Another drawback is that rapid solidification processing is not a commercially attractive method for bulk production.

4. Spray Casting Route

Several attempts are made to successfully integrate the metal powder production step with subsequent powder processing steps in such a way that metal powder is neither produced nor handled at any stage during entire processing, and yet the fundamental principles applied is analogous to those of powder metallurgy route. Spray deposition, also known as spray casting, process consists of atomizing a liquid metal or alloy into very small liquid particles in a specially constructed chamber with a jet of high velocity inert gas. The deposition chamber is simultaneously purged with inert gas to avoid the oxidation of liquid droplets during deposition. The molten metal stream is disintegrated into fine dispersion of droplets. After atomization, the partially solidified droplets are collected on a suitable substrate, which may be stationary, rotating, or oscillating type. It may be either flat or mould type. The droplets travel a predetermined distance prior to impingement on a substrate. Each deposited layer forms the effective substrate for the next layer. The process of deposition of droplets on the substrate occurs until the stream of liquid metal continues. Finally, droplets coalesce and solidify to form a casting, also known as preform. The condition of the substrate would determine, whether the deposit is adherent to it or not. A rough surface would result in the adherence of deposit to the substrate. From a smooth surface substrate, the deposit can be easily removed. The spray deposit may contain porosity, depending upon the process parameters. Hence, the deposit is subjected to mechanical working process, such as rolling and forging to produce finished products. For preparing strip shape preform, a flat substrate is used. The principle of spray deposition was pioneered during 1970s by A.R.E. Singer, at the University College of Swansea, U.K [43].

Figure 10 shows a typical experimental set-up of spray deposition process [44]. An important feature of the spray deposition process is that the metal particles after atomization are used as soon as they are formed, and the metal is not handled in the powder form, and yet it has all the advantages of powder metallurgy route for making metal strip. Further, the spray deposition is insensitive to particle shape. Particle size

and size distribution is of far less importance than in powder metallurgy route. The thickness of the as-deposited strip, known as "green" strip, can be varied within wide limits by adjusting the speed of the substrate in a continuous operation, while maintaining a constant rate of pouring. Segregation is virtually absent in spray deposited strip because all the liquid droplets will have the same composition.

A wide range of materials, including aluminum base alloys, copper base alloys, nickel base alloys, nickel base super-alloys, tool steels, and alloy steels have been processed by spray deposition method. A limited work is reported on the preparation of Cu-Al-Ni SMA by spray casting route. Recently, Cava et at. [45] has reported the spray atomization of Cu-Al-Ni-Mn SMA with nitrogen gas under 0.5 MPa of pressure and a gas metal ratio of 1.93 wherein the precursors were melted and then spray-deposited on a steel substrate rotating at a speed of 60 rpm and positioned 350 mm below the gas nozzle. The resultant Cu-11.85Al-3.2Ni-3Mn SMA exhibited equi-axial grains with monoclinic martensite with a grain size varying from 15 μm to 180 μm moving from bottom to the peripheral region of the spray deposit. It is also reported that the spray forming is an efficient processing route for copper alloys exhibiting SME as the harmful effects of oxidation of the deposit was virtually absent and adjustment of processing parameter can produce the deposits with refined grains. However, no study is made on the mechanical properties of the alloy. The spray forming process is carried out by pouring the liquid metal slowly through a bore nozzle into a conical tundish and with a jet of inert gas, the stream of liquid metal is atomized into droplets of different sizes, which travel downwards and are impinged onto a substrate where it is collected and solidified into a coherent and fully dense deposit pan-cake shape preform. The porosity in the spray deposited Cu-Al-Ni-Mn strip was studied by carrying out the quantitative analysis of the samples under scanning electron microscope. It was observed that on the thickness cross-section, the porosity in the deposit varies with the thickness of the deposit. It is reported that the bottom area of the spray deposited Cu-Al-Ni-Mn strip has relatively large amounts of porosity followed by central and top area regions.

To explain the presence of porosity in the spray deposit, it is necessary to discuss the sequence of events occurring during the deposition process. When the liquid stream

reaches the geometric point of the atomiser, it gets disintegrated and a spray of droplets of different size is created. During the flight, fine size droplets would solidify, while the coarse size droplets may remain in either fully liquid or solid-liquid state. Thus, the spray reaching the deposition surface consists of a mixture of fully solid, fully liquid and solid-liquid particles. The proportion of these types of droplets reaching the substrate would depend on process parameters, such as gas pressure, flight distance, gas to metal ratio, etc. The state of the particles at the time of impingement on the substrate surface would affect the microstructure, and hence the porosity, of the spray deposit. Further, the nature of the substrate changes during deposition. In this study, initially a steel surface acted as a substrate. For subsequent deposition, the immediately deposited layer act as the substrate. The porosity developed in the spray deposit would also depend on the state of the substrate at the time of deposition.

The state of the top surface of the deposit at any instance of deposition process would depend on the heat transfer characteristics present in the system. Two situations may arise. Firstly, the top surface of the spray deposit is fully solid or contains a very thin layer of liquid prior to deposition of the next layer of spray. Secondly, there is a relatively large amount of liquid fraction present on the top surface. As a result, the solidification rate decreases. The droplets reaching the substrate intermingle with the preceding layer of deposit. Consequently, the packing, between the incoming layer of deposit and the preceding layer of deposit, is improved and less amounts of porosity is formed. Heat transfer from the top surface of the spray deposit involves radiation and convection mechanisms. The state of the top layer of the spray deposit would also depend on the heat transfer coefficient at the preform/substrate interface.

Another factor affecting the heat transfer from the spray deposit, via substrate cooling is the thickness of the substrate. A thin substrate would lead to rapid increase of the substrate temperature during initial stages. This would decrease the heat transfer. It has been shown for the spray deposition of thin AISI 1026 strip that the temperature of the top surface of the substrate increases with deposition time (Figure 11.b), and hence with the thickness of spray deposit [46]. In the beginning of deposition, since the substrate is at room temperature, the deposit solidifies quickly due to the severe cooling

on impingement with the substrate surface. The solidification of the deposit may take place both by gas cooling and substrate cooling. The substrate extracts heat at a much faster rate during initial stage of deposition; as a result, the droplets solidify quickly. This results in poor packing and a higher amount of porosity in the bottom area of the spray deposit as shown in Figure 11.a. With the increase in deposition time and hence the deposit thickness, the temperature of the top surface of the preceding layer of deposit increases. As a result, the amount of liquid present on the top layer of the deposit increases with increase in thickness, thus the amounts of porosity decrease with thickness. This explains the presence of relatively higher amounts of porosity in the bottom area of the spray deposit and the decrease in porosity from the bottom towards the top area of the deposit.

Recently, the application of selective laser melting for preparation of Cu-Al-Ni SMA is found to be a promising technique. The selective laser melting method is an additive manufacturing technique that uses high energy laser to melt wherein the metallic powder particles are fused together in a non-equilibrium state to develop intricate parts with refined microstructure. Tomochika et al. [47] applied the reactive gas laser atomization method to produce NiTi alloy coatings using high pressure argon gas on an aluminum base substrate. Authors have reported that the oxygen concentration in the powders of the coating layers has improved the resultant materials properties. Smith et al [48] used vacuum plasma spray forming method to deposit and consolidate pre-alloyed NiTi and NiTiPd powders into near net shape actuators. The process resulted in near net shape deposited material with eliminated porosity and exhibits an excellent shape memory effect. However, the desired transformation temperatures were not achieved due to the variation in the composition of the starting powder and interaction of Ti with oxygen during the process. Mazzer et al. [49] and Gargarella et al [50] combined powder atomization and selective laser melting technique to produce Cu-Al-Ni-Mn SMA by melting the Cu-11.85Al-3.2Ni-3Mn (wt%) master alloy in induction furnace and subsequently atomizing it into powder particles using nitrogen gas atomization. The powder atomization is combined with laser Nd-YAG which subsequently produced the rods with 3 mm diameter and 10 mm in length onto a Cu-10Sn substrate in an inert gas

atmosphere with a relative density of more than 92% and exhibited an average grain size of 32 µm.

Summary

Table 1 summarizes the State of the art for the preparation of Cu-Al-Ni Shape memory alloy. The conventional casting method for preparing Cu-Al-Ni shape memory alloy suffers from a disadvantage that it produces coarse grain structure of the order of ~ 1 mm and is prone to brittle fracture [51]. Therefore, the brittleness is a severe problem in cast Cu-Al-Ni alloys due to large grain size combined with large elastic anisotropy. Several efforts are made in developing fine grained Cu-Al-Ni shape memory alloys with improved mechanical properties. Casting using addition of quaternary element such as Ti, Zr, V and B have shown a significant grain refinement and improvement in the mechanical properties of the Cu-Al-Ni shape memory alloy. When a second phase is present in the matrix phase, the grain growth is hindered because of the grain boundary pinning caused due to the interaction of the grain boundary with the particle. However, compositional control during casting and limitations to achieve the desired level of grain size restricted further development of the alloy. Moreover, hot working of the cast Cu-Al-Ni alloy are attempted to reduce the grain size, which would temporarily reduce the grain size, however recrystallization and grain growth during a properly controlled homogenization stage reduces the final mechanical property of the alloy. Therefore, there is a need to retain the high temperature deformation structure by retarding the effect of recrystallization by immediately quenching the hot rolled samples after the final rolling pass. This would result in the formation of fully martensitic structure which reduces the grain growth coupled with increased mechanical property of alloys.

Rapid solidification processing, on the other hand, offers a convenient and economical route combined with the possibility of improving the mechanical properties of Cu-Al-Ni shape memory alloys [16, 39-42]. However, the rapid solidification processing suffers from a disadvantage that it introduces internal stresses in the material which can impede the growth of the martensitic plates. This effect deteriorates the shape memory properties of the alloy processed by rapid solidification processing. Moreover, the rapid solidification processing is not a commercially attractive method for bulk production.

Powder metallurgy route has emerged as an important alternative to the conventional casting route for preparing Cu-Al-Ni shape memory alloy strips. The powder metallurgy route has potential to reduce the energy requirements and capital equipment costs. The starting materials for powder metallurgy route for preparing Cu-Al-Ni shape memory alloy strips are mixtures of elemental Cu, Al, Ni powders or pre-alloyed Cu-Al-Ni powder [30, 31]. The pre-alloyed Cu-Al-Ni powder can be obtained either by inert gas atomization or mechanical alloying. The pre-alloyed Cu-Al-Ni powder reduces the sintering time. The powder metallurgy route starting from elemental powder mixture suffers from a disadvantage of chemical homogeneity. On the other hand, the powder metallurgy route based on mechanical alloying offers better chemical homogeneity, achieves the near net shape products and produces fine-grained materials. However, the requirement of an inert atmosphere during the milling of elemental Cu, Al and Ni powders, and prolonged milling time make the process commercially unattractive. The serious problem with the milling process is that it leads to contamination from the debris of the vials and balls during milling of the powder [56]. The contamination typically observed during the ball milling process is primarily due to the attrition of vials and balls which gets associated along with metal powders. Terayama et al. [57] has reported the inclusion of Fe and Cr from the vial walls as the major contaminant during the mechanical alloying of Ni-Ti SMA. Vajpai and Dube et al [58] has also reported the possibility of contamination by process control agent during the mechanical alloying of 80Ni-20Fe powder particles. However, the small amount of contamination due to steel balls has no effect in this alloy since it contained 20 wt%. of Fe. Further, Vajpai et al. [59] has also reported that prolonged milling hours leads to contamination and formation of small alumina particles which causes pinning effect in the grain boundaries of Cu-Al-Ni SMA. Usually, the contamination lead to inferior shape recovery behavior of the final material. Therefore, use of suitable milling container, balls and avoiding the prolonged milling hours could be a better alternative to avoid contamination [60]. However, the commercial application of powder metallurgy has been hindered, primarily due to the higher cost of starting metal powders.

Few work on preparing Cu-Al-Ni shape memory alloy via spray deposition route wherein the powder production step is integrated with subsequent powder processing steps

such that metal powder was neither produced nor handled at any intermediate processing steps, and yet the fundamental principles applied is like those of powder metallurgy route. Details of the subsequent mechanical working process is not discussed. A possible way to decrease the grain size of the Cu-Al-Ni strip prepared by spray deposition – hot rolling route could be to atomize the melt by a gas jet containing some amount of oxygen. This would lead to the introduction of fine sized Al_2O_3 particles in the finished product, which will restrict the grain growth. It is expected that such a process methodology would produce fine grain size Cu-Al-Ni strip via spray deposition – hot rolling route. The additive manufacturing such as selective laser melting technique is found promising and emerging in preparation of Cu-Al-Ni alloy with refined microstructure.

ACKNOWLEDGMENT

ORCID

Ashish Agrawal http://orcid.org/0000-0002-5550-0147

References

1. T. Tadaki: "Cu-based shape memory alloys" in 'Shape memory materials', (ed. K. Otsuka and C. M. Wayman), 97–116; 1998, Cambridge, Cambridge Univesity Press

2. M.H. Wu in: T.W. Duerig, K. N. Melton, D. Stockel and C. M. Wayman: "Engineering Aspects of Shape memory alloys", (1990), Butterworth-Heinemann Ltd., London.

3. Dimitris C. Lagoudas, Shape Memory Alloys (2008), Berlin: Springer.

4. K. Otsuka and K. Shimizu: Jpn. J. Appl. Phys., 1969, vol.8, no. 10, pp. 1196-1204.

5. K. Otsuka and K. Shimizu: Scr. Metall., 1970, vol. 4, pp. 469-472.

6. K. Otsuka: Jpn. J. Appl. Phys., vol. 10, no. 5, 1971.

7. A. Sato, E. Chishima, K. Soma and T. Mori: Acta. Metall., 1982, vol. 30, pp. 1177-1183.

8. http://en.wikipedia.org/wiki/Shape_memory_alloy

9. S. Miyazaki, K. Otsuka: ISIJ International, 1989, vol. 29, no. 5, pp. 353-377.

10. R.E. Reed Hill: Physical Metallurgy Principles, 3rd Edition, PWS-KENT Pub. Co., Boston, 1992.

11. http://en.wikipedia.org/wiki/Martensite

12. J.V. Humbeeck, M. Chandrasekaran and L. Delaey, Endeavour, New Series, 15, No.4, (1991), 148.

13. http://www.copper.org/publications/newsletters/innovations/1999/07/shape.html

14. T.W. Duerig: Materials Science Forum, 1990, Vol-56-58, pp. 679-692.

15. http://www.eggshell-robotics.com/blog/44-inchworm-robot

16. G. Lojen, I. Anzel, A. Kneissl, A. Krizman, E. Unterweger , B. Kosec and M. Bizjak: Journal of Materials Processing Technology, 2005, vol. 162-163, pp. 220-229.

17. S.S. Leu, Y. Chen, and R.D. Jean: J. Mater. Sci., 1992, vol. 27, pp. 2792–2798.

18. D. W. Roh, J. W. Kim, T. J. Cho and Y. G. Kim: Materials Science and Engineering A, 1991, 136, pp. 17-23

19. T. W. Duerig, J. Albrecht, and G. H. Gessinger, 'A Shape-Memory Alloy for High-Temperature Applications', JOURNAL OF METALS, 1982, pp. 14-20

20. G.N. Sure and L.C. Brown: Metall. Trans A, 1984, vol 15, pp. 1613-1621.

21. K. Oishi and L.C. Brown: Metall. Trans. A, 1971, vol. 2, pp. 1971-1977.

22. K. Mukunthan and L.C. Brown: Metall. Trans. A, 1988, vol. 19, pp. 2921-2929.

23. J.L.L. Gama, C.C. Dantas, N.F. Quadros, R.A.S. Ferreira and Y.P. Yadava, 'Microstructure-Mechanical Property Relationship to Copper Alloys with Shape Memory during thermomechanical Treatments', Metallurgical and Materials Transactions A, 37a, 2006, 77-87

24. Dr. M.K. Abbass, Dr. M.M. Al-Kubaisy, R.S.A. Adnan, 'The Effect of Thermo-Mechanical Treatment on Mechanical Properties & Microstructure for (Cu-Al-Ni) Shape Memory Alloy' Eng. & Tech.Journal, Vol.34,Part (A), No.13,2016, pp- 2518-2526

25. J.S. Lee, C.M. Wayman, Trans. Jpn. Inst. Met. 27 (1986) 584–591.

26. S.N. Saud, E. Hamzah, T. Abubakar, M. Zamri, M. Tanemura, 'Influence of Ti additions on the martensitic phase transformation and mechanical properties of Cu–Al–Ni shape memory alloys', 2014, J Therm Anal Calorim (2014) 118:111–122

27. S.N. Saud, T.A.A. Bakar, E. Hamzah, M. K. Ibrahim and A. Bahador, 'Effect of Quarterly Element Addition of Cobalt on Phase Transformation Characteristics of Cu-Al-Ni Shape Memory Alloys', Metallurgical And Materials Transactions A, 2015, 46A, pp. 3528-3542

28. M.K. Abbass, M.M. Radhi, R.S.A. Adnan, 'The effect of Germanium addition on mechanical properties & microstructure of Cu-Al-Ni shape memory alloy', 5th International Conference of Materials Processing and Characterization (ICMPC 2016), Materials Today: Proceedings 4 (2017) 224–233

29. R.K. Dube: International Materials Review, 1990, vol. 35, pp. 253-292.

30. S.M. Tang, C.Y. Chung, and W.G. Liu, J. Mater. Proc. Tech., 1997, vol. 63, pp. 307-312.

31. P. P. Rodriguez, A. Ibarra, A. Iza-Mendia, V. Recarte, J. I. Perez-Landazabal, J. San Juan and M. L. No, Mater. Sci. and Eng. A, 2004, vol. 378, no. 1-2, pp. 263-268.

32. Z. Xiao, Z. Li, M. Fang, S. Xiong, X. Sheng, M. Zhou, 'Effect of processing of mechanical alloying and powder Metallurgy On Microstructure And Properties Of Cu–Al–Ni–Mn Alloy', Materials Science and Engineering A 488 (2008) 266–272

33. A. Ibarra, P.P. Rodriguez, V. Recarte, J.I. Perez-Landazabal, M.L. No and J. SanJuan, Material Science and Engineering A, 370, (2004). pp. 492-496.

34. A.F. Dericioglu, B. Ögel and Ş, Bor, 'Production of Cu-Zn-Al Shape Memory Alloys by Powder Metallurgy from Elemental Powders', in 'Materials Development and Processing - Bulk Amorphous Materials, Undercooling and Powder Metallurgy, (ed. Prof. J. V. Wood, Prof. Dr. L. Schultz and Prof. Dr. D. M. Herlach), Vol. 8, 2006, Wiley-VCH Verlag GmbH, 10.1002/3527607277.ch55

35. S. K. Vajpai, R. K. Dube M. Sharma, 'Studies on the mechanism of the structural evolution in Cu–Al–Ni elemental powder mixture during high energy ball milling', J Mater Sci (2009) 44:4334–4341

36. M. Sharma, S.K. Vajpai and R.K. Dube, 'Processing and Characterization of Cu-Al-Ni Shape Memory Alloy Strips Prepared from Elemental Powders via a Novel Powder Metallurgy Route', Metallurgical and Materials Transactions A, 2010, 41A, 2905–2913.

37. M. Sharma, S. K. Vajpai and R. K. Dube, 'Synthesis and properties of Cu–Al–Ni shape, memory alloy strips prepared via hot densification rolling of powder preforms', Powder Metallurgy, 2011, Vol. 54, no. 5, pp.620-627.

38. S.K. Vajpai, R.K. Dube, S. Sangal, 'Microstructure and properties of Cu–Al–Ni shape memory alloy strips prepared via hot densification rolling of argon atomized powder preforms', Materials Science and Engineering A 529 (2011) 378– 387

39. H. Morawiec, J. Lelatko, D. Stroz, M. Gigla: Mater. Sci. Eng. A, vol. 273–275, 1999, pp. 708–712.

40. T. Goryczka, H. Morawiec: Mater. Sci. Eng. A, 2004, vol. 378, pp. 248-252.

41. J. Malarria, C. Elgoyhen, Ph. Vermaut, P. Ochin, R. Portier: Mater. Sci. Eng. A, 2006, vol. 438-440, pp. 763-767.

42. C. Sobrero, R. Bolmaro, J. Malarria, P. Ochin, R. Portier: Mater. Sci. Eng. A, 2008, vol. 481–482, pp. 688-692.

43. Singer et al.; Method of forming composite metal strip, US Patent No. 3775156, 1973

44. K.K Sahu, R.K. Dube, S.C. Koria: Journal of Powder Metallurgy, 2009, vol. 52, no. 2, pp. 135-144.

45. R.D. Cava, C. Bolfarini, C.S. Kiminami, E.M. Mazzer, W.J.B Filho, P. Gargarella, J. Eckert, 'Spray forming of Cu–11.85Al–3.2Ni–3Mn (wt%) shape memory alloy', Journal of Alloys and Compounds 615 (2014) S602–S606

46. S. Annavarapu, D. Apelian, A. Lawley, Metall. Trans. A, Vol. 21, No. 12, 1990, pp. 3237-3256.

47. H. Tomochika, H. Kikuchi, T. Araki and M. Nishida, Fabrication of NiTi intermetallic compound by a reactive gas laser atomization process, Materials Science and Engineering A356 (2003), pp. 122-129

48. R. Smith, J. Mabe, R. Ruggeri, and R. Noebe, Spray forming of NiTi and NiTiPd shape-memory alloys, Industrial and Commercial Applications of Smart Structures Technologies (2008), Proc. of SPIE Vol. 6930, doi: 10.1117/12.775243

49. EM Mazzer, CS Kiminami, P. Gargarella, RD Cava, LA Basilio, C. Bolfarini, Atomization and selective laser melting of a Cu-Al-Ni-Mn shape memory alloy. Materials Science Forum. 2014; 802:343-348. http://dx.doi.org/10.4028/www.scientific. net/MSF.802.343.

50. P. Gargarella, CS Kiminami, EM Mazzer, RD Cava, LA Basilio, C. Bolfarini, WJ Botta, J. Eckert, T. Gustmann and S. Pauly, Phase formation, thermal stability and mechanical properties of a Cu-Al-Ni-Mn shape memory alloy prepared by selective laser melting, Materials Research, DOI: http://dx.doi.org/10.1590/1516-1439.338914

51. U. Sari and T. Kirindi, Effect of deformation on microstructure and mechanical properties of a Cu-Al-Ni shape memory alloy, Materials characterization, (2008), 59: 920-929

52. U. Sari, I. Aksoy, Journal of Material processing technology, 195, (2008), pp. 920-929.

53. S.K,Vajpai, R.K.Dube and S.Sangal, Effect of rapid solidification powder metallurgy processing to prepare Cu-Al-Ni high temperature shape memory alloy strips with high strength and high ductility, Materials Science and Engineering A, 570 (2013), 32-42

54. R. Rajeshkumar and Dr. T.Vigraman, Formation of Cu-Al-Ni shape memory alloy with the addition of alloying elements Mn and Si, International journal of scientific and engineering research, (2014), vol. 5, issue 5, 179-182

55. Z. Li, Z.Y. Pan, N. Tang, Y.B. Jiang, N. Liu, M. Fang, F. Zheng, Cu-Al-Ni-Mn shape memory alloy processed by mechanical alloying and powder metallurgy Materials Science and Engineering A 417 (2006) 225–229

56. C. Suryanarayana, Mechanical alloying and milling. Progress in Materials Science 46, (2001), 1–184.

57. A. Terayama, H. Kyogoku, M. Sakamura and S. Komatsu, Fabrication of TiNi powder by mechanical alloying and shape memory characteristics of the sintered alloy, Mater. Trans., 2006, 47, 550–557.

58. S. K. Vajpai and R. K. Dube, Preparation of nanocrystalline Ni–Fe strip via mechanical alloying–compaction–sintering–hot rolling route, J Mater Sci (2009) 44:129–135, DOI 10.1007/s10853-008-3111-2

59. S. K. Vajpai, R. K. Dube, P. Chatterjee and S. Sangal, A novel powder metallurgy approach to prepare fine-grained Cu-Al-Ni shape-memory alloy strips from elemental powders, Metallurgical and materials transactions 43A, (2012), 2482-2499

60. M. Shafeeq, G. K. Gupta, Hirshikesh, M. M. Malik and O. P. Modi, Effect of milling parameters on processing, microstructure and properties of Cu–Al–Ni–Ti shape memory alloys, Powder metallurgy (2015), Vol. 58, issue 4, pp. 265-272,

Processing route Average grain size (mm) Average fracture	Average grain size (µm)	Average fracture stress (MPa)	Average fracture strain (%)	Reference
Polycrystals: Conventional casting without quaternary alloying	20	550	5	12
	750	150	2	12
	260	380	4	18
	1500	440	0.6	23
	250	650	5	11
	460	260	0.8	21
	200	-	2.6	21
	-	240	1	9
	600-1900	605	7.3	51
	1400	881	8	52
Polycrystals: Conventional casting with quaternary alloying	15	930	7	12
	50	425	4	12
	80	532	2.2	21
	90	830	7.5	18
	116	903	8.6	19
	350	952	15	52
Polycrystals: Powder metallurgy (PM)	20	800	6	23
	30	576	5.25	20
	30	749	6.7	21
	100	470	12.6	22
	90	530	12.3	25
	27	626	13.5	24
	6	677	13.1	26
	16	810	12	53
	20	308	-	54
	3	-	-	55
Rapid Solidification Process	20-50	-	4.4	40
	<2	-	1.8	41
Spray Deposition	15-180	-	-	45

Table 1: State of the art for the preparation of Cu-Al-Ni Shape memory alloy
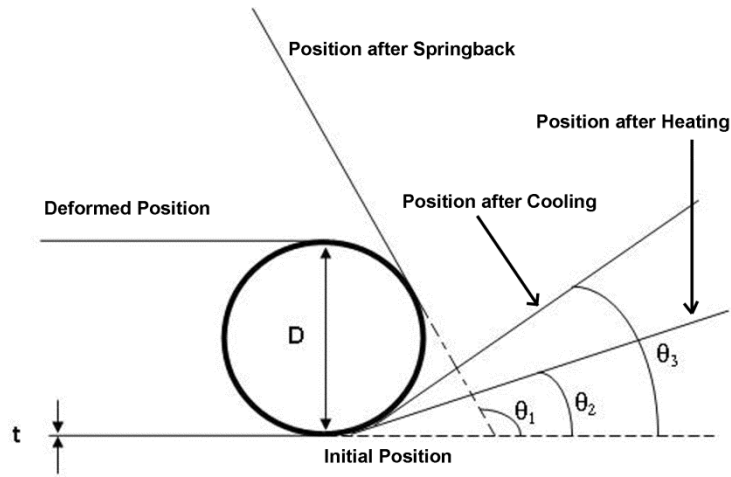
Figure 1: Schematic diagram of shape memory effect testing arrangement. [38]
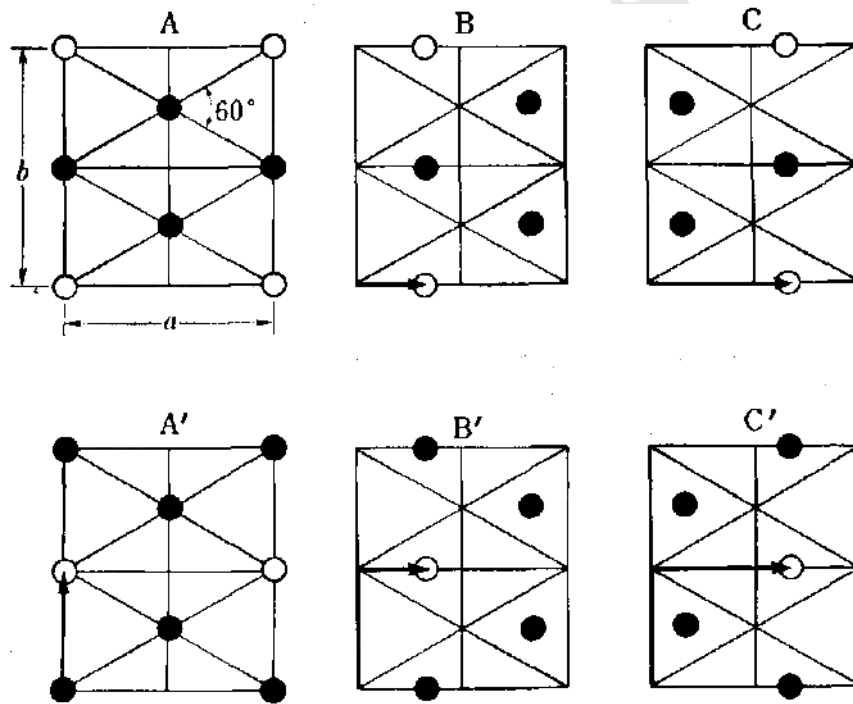
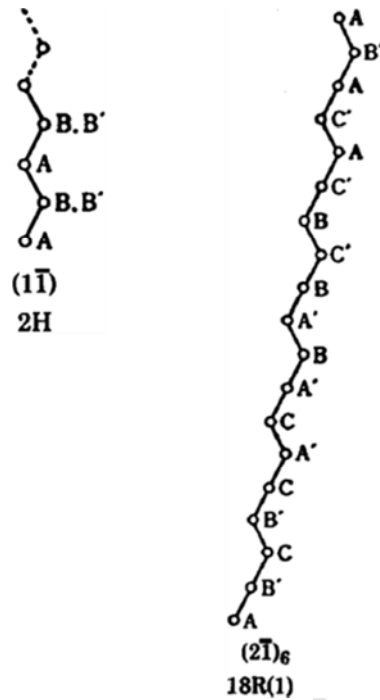**Figure 2:** Six types of planes of martensite formed from DO_3 type parent phase [10].

B.B'
A
B.B'
A
(1$\bar{1}$)
2H

A
B'
A
C'
A
C'
B
C'
B
A'
B
A'
C
A'
C
B'
C
B'
A
(2$\bar{1}$)$_6$
18R(1)

**Figure 3:** Stacking sequence of the planes in 2H and 18R martensites [10].

Austenite
- High temperature phase
- Cubic crystal structure
Martensite
- Low temperature phase
- Monoclinic crystal structure

Austenite

Heating

A_f
A_s
M_s
M_f

Cooling

Twinned martensite   Deformed martensite

Loading

Load

Temperature
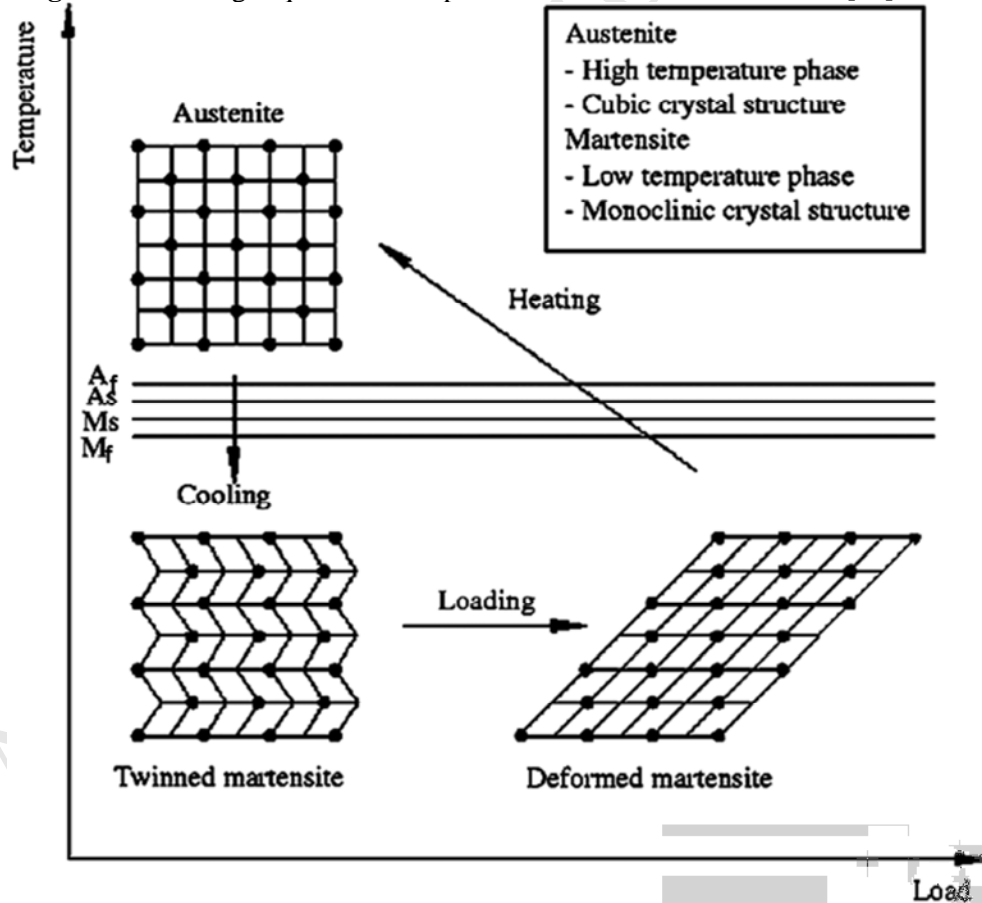
Figure 4: Shape memory effect at an atomic level [14].
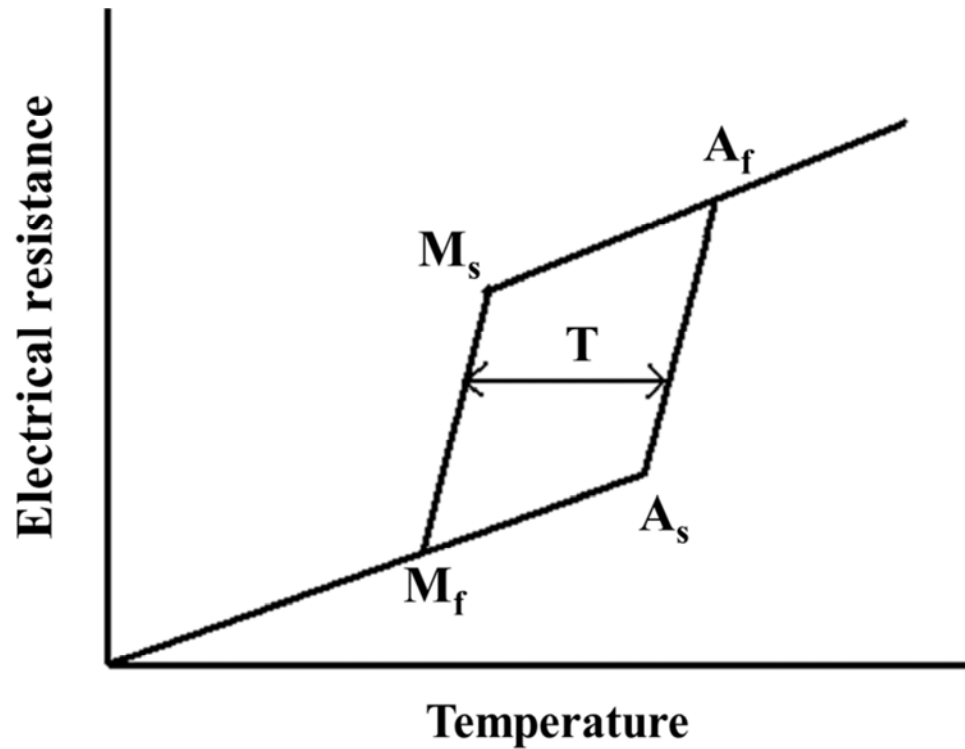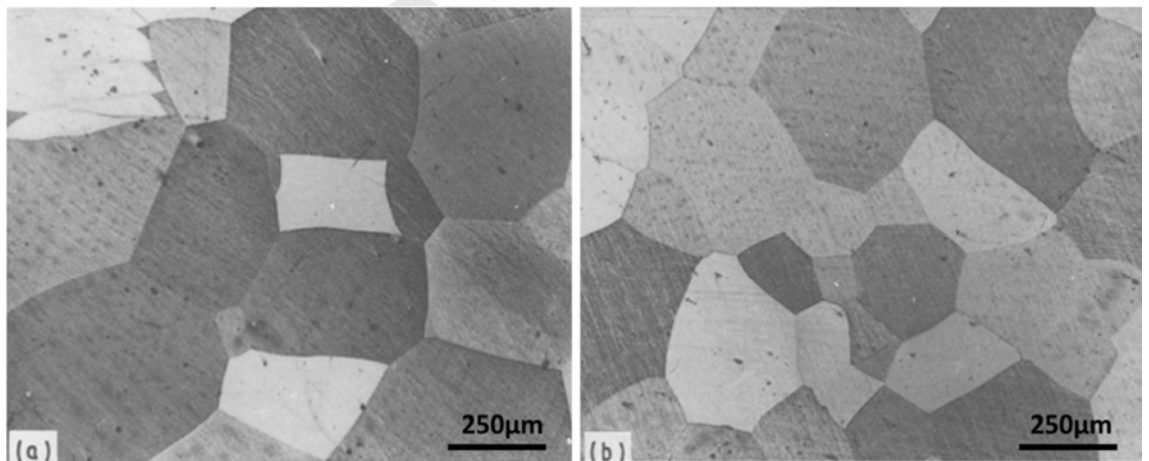
**Figure 5:** A typical hysteresis curve of a shape memory alloy [15].
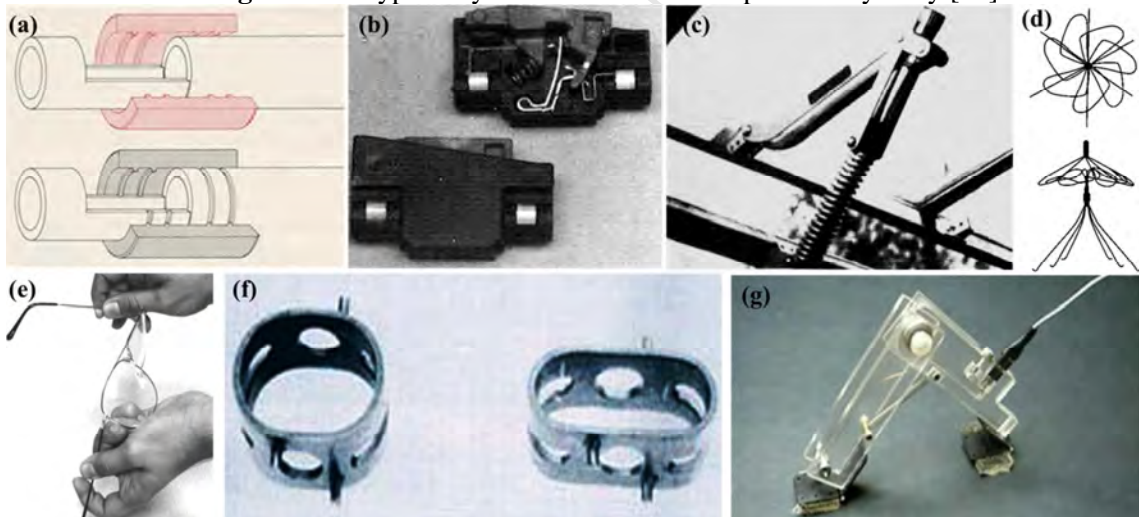
Figure 6: Applications of shape memory alloys: (a) Hydraulic tube-couplings (b) Electric circuit breaker, (c) thermal actuator, (d) Simon filter, (e) eye glass frame, (f) spacer and (g) robotic arm [2, 16-17].
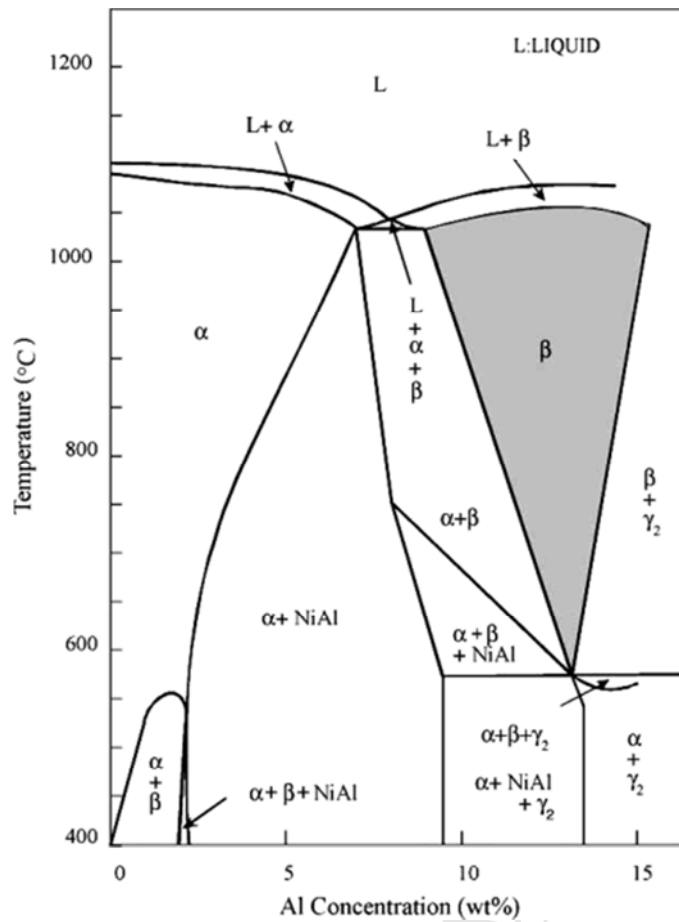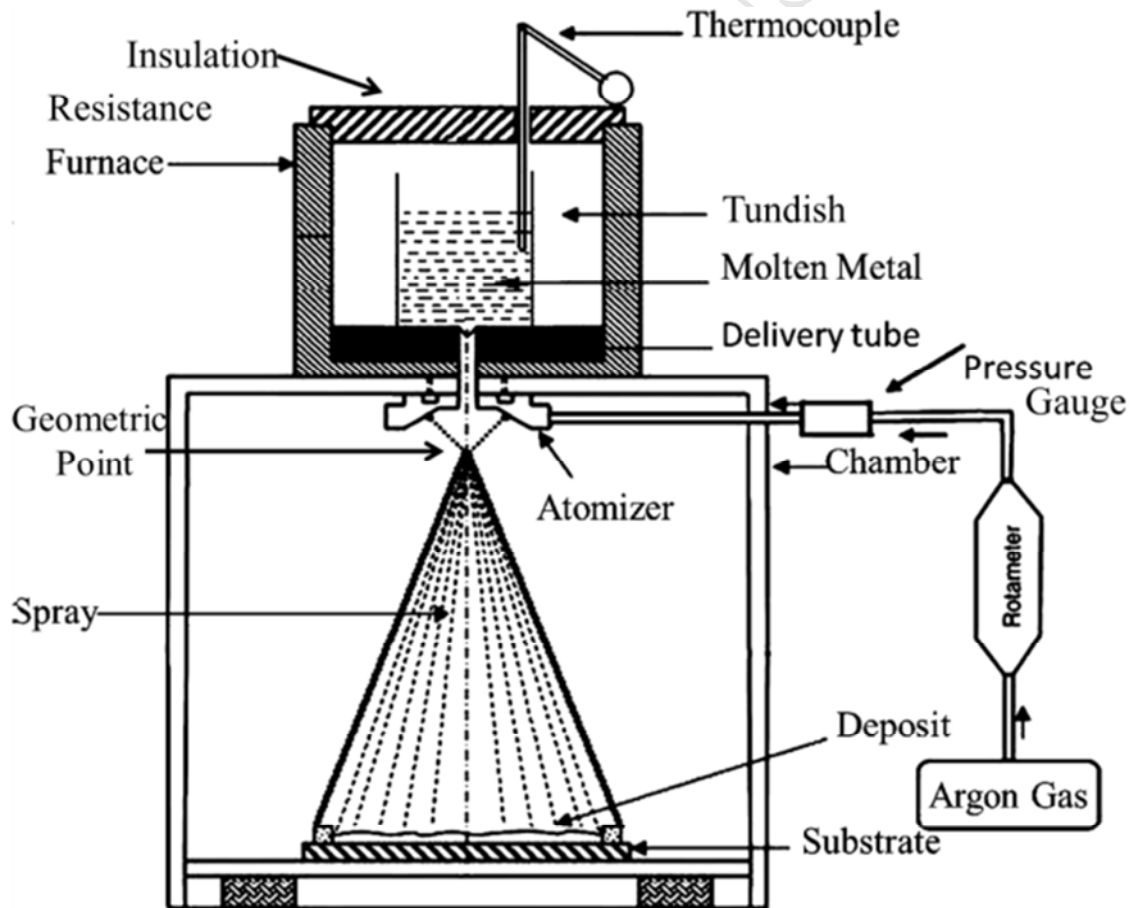
Figure 7: Phase diagram of the Cu-Al-Ni ternary alloy system with 3 wt % Ni [16].


Figure 8: Typical SEM microstructures of the Cu-13.8Al-3.8Ni (wt %) and Cu-13.8Al-4Ni-0.2Cr (wt %) obtained after solution treatment at 850 ˚C followed by water quenching [17].
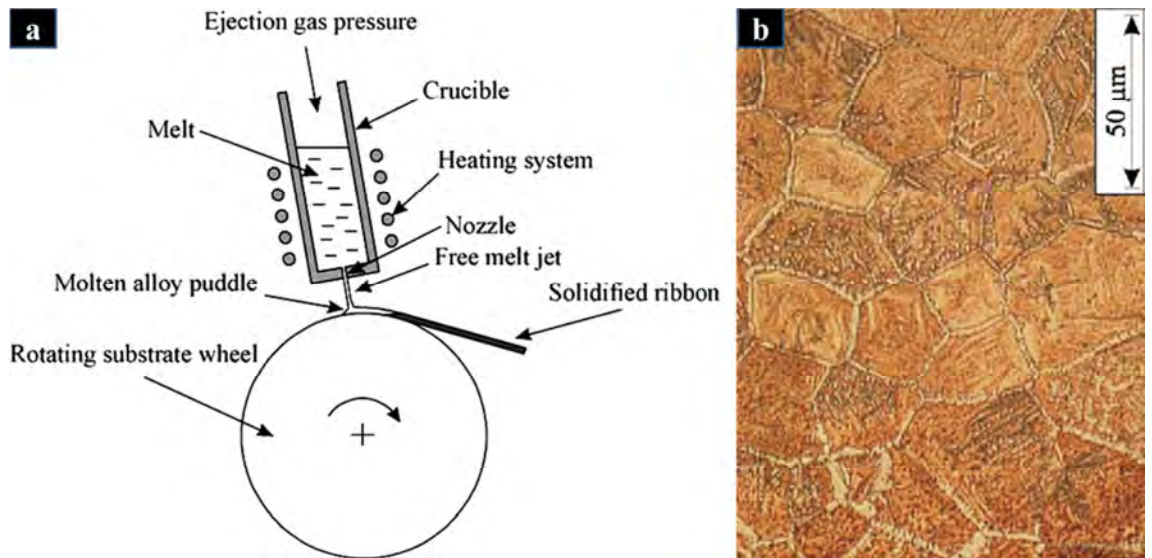
Figure 9: (a) Experimental set-up of a free jet melt spinner and (b) Microstructure obtained in the rapidly solidified Cu-Al-Ni alloy [16].

Figure 10: Experimental set-up of the spray atomization and deposition unit [44]
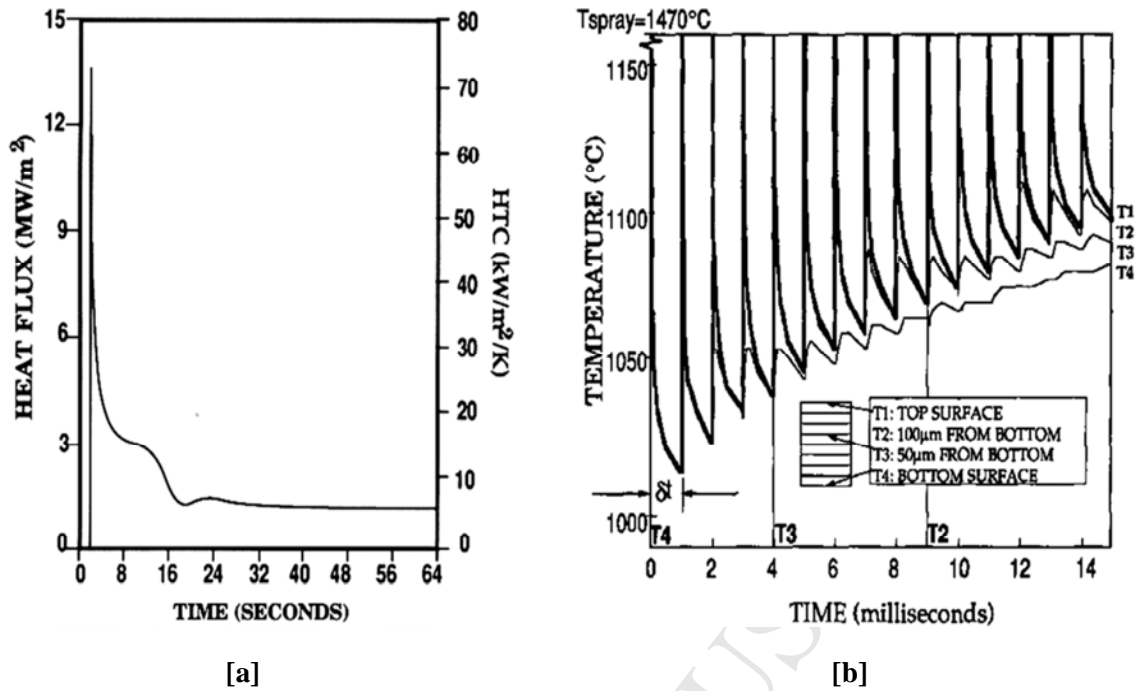
[a]   [b]

Figure 11: (a) Variation of heat flux from the deposit into the substrate and the heat transfer coefficient at the deposit/substrate interface as a function of the deposition time and (b) Thermal histories at selected locations predicted by the discrete event formulation [45].